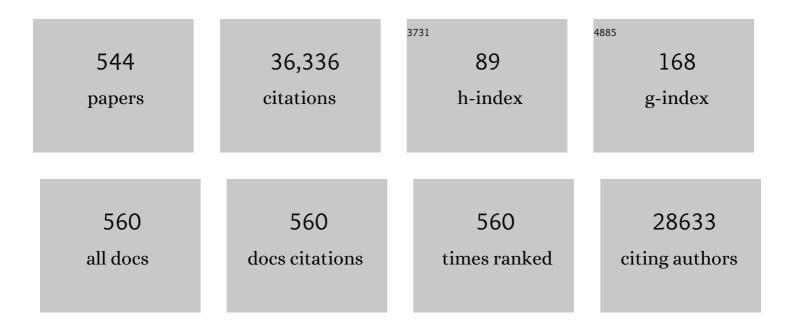
Yi-Bing Cheng

List of Publications by Year in descending order

Source: https://exaly.com/author-pdf/7470154/publications.pdf Version: 2024-02-01



#	Article	IF	CITATIONS
1	A Fast Deposition rystallization Procedure for Highly Efficient Lead Iodide Perovskite Thinâ€Film Solar Cells. Angewandte Chemie - International Edition, 2014, 53, 9898-9903.	13.8	1,292
2	Mesoporous Anatase TiO ₂ Beads with High Surface Areas and Controllable Pore Sizes: A Superior Candidate for Highâ€Performance Dyeâ€Sensitized Solar Cells. Advanced Materials, 2009, 21, 2206-2210.	21.0	926
3	Degradation observations of encapsulated planar CH ₃ NH ₃ PbI ₃ perovskite solar cells at high temperatures and humidity. Journal of Materials Chemistry A, 2015, 3, 8139-8147.	10.3	874
4	Consensus statement for stability assessment and reporting for perovskite photovoltaics based on ISOS procedures. Nature Energy, 2020, 5, 35-49.	39.5	797
5	Thin-film Sb2Se3 photovoltaics with oriented one-dimensional ribbons and benign grain boundaries. Nature Photonics, 2015, 9, 409-415.	31.4	781
6	Universal passivation strategy to slot-die printed SnO2 for hysteresis-free efficient flexible perovskite solar module. Nature Communications, 2018, 9, 4609.	12.8	596
7	Highly efficient photocathodes for dye-sensitized tandem solar cells. Nature Materials, 2010, 9, 31-35.	27.5	585
8	Gas-assisted preparation of lead iodide perovskite films consisting of a monolayer of single crystalline grains for high efficiency planar solar cells. Nano Energy, 2014, 10, 10-18.	16.0	504
9	Resistance of alkali-activated slag concrete to acid attack. Cement and Concrete Research, 2003, 33, 1607-1611.	11.0	465
10	Rubidium Multication Perovskite with Optimized Bandgap for Perovskiteâ€ s ilicon Tandem with over 26% Efficiency. Advanced Energy Materials, 2017, 7, 1700228.	19.5	443
11	Functionalization of perovskite thin films with moisture-tolerant molecules. Nature Energy, 2016, 1, .	39.5	439
12	A novel quadruple-cation absorber for universal hysteresis elimination for high efficiency and stable perovskite solar cells. Energy and Environmental Science, 2017, 10, 2509-2515.	30.8	437
13	Benefit of Grain Boundaries in Organic–Inorganic Halide Planar Perovskite Solar Cells. Journal of Physical Chemistry Letters, 2015, 6, 875-880.	4.6	422
14	Dye-Sensitized Solar Cells Employing a Single Film of Mesoporous TiO ₂ Beads Achieve Power Conversion Efficiencies Over 10%. ACS Nano, 2010, 4, 4420-4425.	14.6	412
15	Synthesis of Monodisperse Mesoporous Titania Beads with Controllable Diameter, High Surface Areas, and Variable Pore Diameters (14â^23 nm). Journal of the American Chemical Society, 2010, 132, 4438-4444.	13.7	405
16	Dualâ€Function Scattering Layer of Submicrometerâ€Sized Mesoporous TiO ₂ Beads for Highâ€Efficiency Dyeâ€Sensitized Solar Cells. Advanced Functional Materials, 2010, 20, 1301-1305.	14.9	385
17	Understanding of perovskite crystal growth and film formation in scalable deposition processes. Chemical Society Reviews, 2020, 49, 1653-1687.	38.1	364
18	Highly Efficient Blueâ€Emitting Biâ€Doped Cs ₂ SnCl ₆ Perovskite Variant: Photoluminescence Induced by Impurity Doping. Advanced Functional Materials, 2018, 28, 1801131.	14.9	358

#	Article	IF	CITATIONS
19	Lead halide–templated crystallization of methylamine-free perovskite for efficient photovoltaic modules. Science, 2021, 372, 1327-1332.	12.6	351
20	Alkali activation of Australian slag cements. Cement and Concrete Research, 1999, 29, 113-120.	11.0	347
21	Acoustic-optical phonon up-conversion and hot-phonon bottleneck in lead-halide perovskites. Nature Communications, 2017, 8, 14120.	12.8	330
22	Sulfate attack on alkali-activated slag concrete. Cement and Concrete Research, 2002, 32, 211-216.	11.0	328
23	Solutionâ€Processed Antimony Selenide Heterojunction Solar Cells. Advanced Energy Materials, 2014, 4, 1301846.	19.5	318
24	Phase Segregation Enhanced Ion Movement in Efficient Inorganic CsPbIBr ₂ Solar Cells. Advanced Energy Materials, 2017, 7, 1700946.	19.5	318
25	Ultra-thin high efficiency semitransparent perovskite solar cells. Nano Energy, 2015, 13, 249-257.	16.0	310
26	Flexible and Semitransparent Organolead Triiodide Perovskite Network Photodetector Arrays with High Stability. Nano Letters, 2015, 15, 7963-7969.	9.1	293
27	Hybrid interfacial layer leads to solid performance improvement of inverted perovskite solar cells. Energy and Environmental Science, 2015, 8, 629-640.	30.8	285
28	Effect of admixtures on properties of alkali-activated slag concrete. Cement and Concrete Research, 2000, 30, 1367-1374.	11.0	284
29	High-performance top-gated monolayer SnS2 field-effect transistors and their integrated logic circuits. Nanoscale, 2013, 5, 9666.	5.6	269
30	Comparison of solution intercalation and melt intercalation of polymer–clay nanocomposites. Polymer, 2002, 43, 4251-4260.	3.8	268
31	Effect of elevated temperature curing on properties of alkali-activated slag concrete. Cement and Concrete Research, 1999, 29, 1619-1625.	11.0	260
32	Copper(I) Iodide as Hole onductor in Planar Perovskite Solar Cells: Probing the Origin of <i>J</i> – <i>V</i> Hysteresis. Advanced Functional Materials, 2015, 25, 5650-5661.	14.9	260
33	Sequential Deposition of CH ₃ NH ₃ PbI ₃ on Planar NiO Film for Efficient Planar Perovskite Solar Cells. ACS Photonics, 2014, 1, 547-553.	6.6	245
34	Copper–Nickel Nitride Nanosheets as Efficient Bifunctional Catalysts for Hydrazineâ€Assisted Electrolytic Hydrogen Production. Advanced Energy Materials, 2019, 9, 1900390.	19.5	243
35	Hybrid Graphene–Perovskite Phototransistors with Ultrahigh Responsivity and Gain. Advanced Optical Materials, 2015, 3, 1389-1396.	7.3	240
36	Synergic Interface Optimization with Green Solvent Engineering in Mixed Perovskite Solar Cells. Advanced Energy Materials, 2017, 7, 1700576.	19.5	240

#	Article	IF	CITATIONS
37	Threeâ€Dimensional Hierarchical GeSe ₂ Nanostructures for High Performance Flexible Allâ€Solidâ€State Supercapacitors. Advanced Materials, 2013, 25, 1479-1486.	21.0	236
38	Encapsulation for improving the lifetime of flexible perovskite solar cells. Nano Energy, 2015, 18, 118-125.	16.0	232
39	Resistance of alkali-activated slag concrete to carbonation. Cement and Concrete Research, 2001, 31, 1277-1283.	11.0	221
40	CH ₃ NH ₃ PbI ₃ -Based Planar Solar Cells with Magnetron-Sputtered Nickel Oxide. ACS Applied Materials & Interfaces, 2014, 6, 22862-22870.	8.0	214
41	Layered Silicate Nanocomposites Based on Various High-Functionality Epoxy Resins:Â The Influence of Cure Temperature on Morphology, Mechanical Properties, and Free Volume. Macromolecules, 2003, 36, 1616-1625.	4.8	209
42	Fabrication of flexible dye sensitized solar cells on plastic substrates. Nano Energy, 2013, 2, 174-189.	16.0	209
43	A Power Pack Based on Organometallic Perovskite Solar Cell and Supercapacitor. ACS Nano, 2015, 9, 1782-1787.	14.6	201
44	Synthesis and Transfer of Large-Area Monolayer WS ₂ Crystals: Moving Toward the Recyclable Use of Sapphire Substrates. ACS Nano, 2015, 9, 6178-6187.	14.6	200
45	Perovskite Tandem Solar Cells. Advanced Energy Materials, 2017, 7, 1602761.	19.5	193
46	Direct observation of intrinsic twin domains in tetragonal CH3NH3PbI3. Nature Communications, 2017, 8, 14547.	12.8	191
47	Nickel oxide nanoparticles for efficient hole transport in p-i-n and n-i-p perovskite solar cells. Journal of Materials Chemistry A, 2017, 5, 6597-6605.	10.3	188
48	Growth, patterning and alignment of organolead iodide perovskite nanowires for optoelectronic devices. Nanoscale, 2015, 7, 4163-4170.	5.6	181
49	Defect trapping states and charge carrier recombination in organic–inorganic halide perovskites. Journal of Materials Chemistry C, 2016, 4, 793-800.	5.5	171
50	Photonics and Optoelectronics of 2D Metalâ€Halide Perovskites. Small, 2018, 14, e1800682.	10.0	168
51	Hydrothermal synthesis of ultrasmall CuCrO2 nanocrystal alternatives to NiO nanoparticles in efficient p-type dye-sensitized solar cells. Journal of Materials Chemistry, 2012, 22, 24760.	6.7	162
52	Selfâ€Adhesive Macroporous Carbon Electrodes for Efficient and Stable Perovskite Solar Cells. Advanced Functional Materials, 2018, 28, 1802985.	14.9	161
53	Dye-sensitized nickel(II)oxide photocathodes for tandem solar cell applications. Nanotechnology, 2008, 19, 295304.	2.6	160
54	Insights into Planar CH ₃ NH ₃ PbI ₃ Perovskite Solar Cells Using Impedance Spectroscopy. Journal of Physical Chemistry C, 2015, 119, 4444-4453.	3.1	160

#	Article	lF	CITATIONS
55	Interfacial benzenethiol modification facilitates charge transfer and improves stability of cm-sized metal halide perovskite solar cells with up to 20% efficiency. Energy and Environmental Science, 2018, 11, 1880-1889.	30.8	148
56	The critical role of composition-dependent intragrain planar defects in the performance of MA1–xFAxPbI3 perovskite solar cells. Nature Energy, 2021, 6, 624-632.	39.5	144
57	Amorphous hole-transporting layer in slot-die coated perovskite solar cells. Nano Energy, 2017, 31, 210-217.	16.0	142
58	p-Type mesoscopic NiO as an active interfacial layer for carbon counter electrode based perovskite solar cells. Dalton Transactions, 2015, 44, 3967-3973.	3.3	138
59	Hierarchical silicon nanowires-carbon textiles matrix as a binder-free anode for high-performance advanced lithium-ion batteries. Scientific Reports, 2013, 3, 1622.	3.3	136
60	Recent progress in hybrid perovskite solar cells based on n-type materials. Journal of Materials Chemistry A, 2017, 5, 10092-10109.	10.3	136
61	Structural engineering using rubidium iodide as a dopant under excess lead iodide conditions for high efficiency and stable perovskites. Nano Energy, 2016, 30, 330-340.	16.0	133
62	Eliminated hysteresis and stabilized power output over 20% in planar heterojunction perovskite solar cells by compositional and surface modifications to the low-temperature-processed TiO ₂ layer. Journal of Materials Chemistry A, 2017, 5, 9402-9411.	10.3	127
63	Light-induced reversal of ion segregation in mixed-halide perovskites. Nature Materials, 2021, 20, 55-61.	27.5	126
64	Formation of TiB2–TiC composites by reactive sintering. Ceramics International, 1999, 25, 353-358.	4.8	121
65	Diammonium and Monoammonium Mixedâ€Organicâ€Cation Perovskites for High Performance Solar Cells with Improved Stability. Advanced Energy Materials, 2017, 7, 1700444.	19.5	121
66	Structural and Chemical Changes to CH ₃ NH ₃ PbI ₃ Induced by Electron and Gallium Ion Beams. Advanced Materials, 2018, 30, e1800629.	21.0	120
67	Thermal stability and flammability of silicone polymer composites. Polymer Degradation and Stability, 2006, 91, 1373-1379.	5.8	119
68	17% efficient printable mesoscopic PIN metal oxide framework perovskite solar cells using cesium-containing triple cation perovskite. Journal of Materials Chemistry A, 2017, 5, 22952-22958.	10.3	119
69	Effect of organo-phosphorus and nano-clay materials on the thermal and fire performance of epoxy resins. Journal of Applied Polymer Science, 2004, 91, 1233-1253.	2.6	118
70	[6,6]-Phenyl-C ₆₁ -Butyric Acid Methyl Ester/Cerium Oxide Bilayer Structure as Efficient and Stable Electron Transport Layer for Inverted Perovskite Solar Cells. ACS Nano, 2018, 12, 2403-2414.	14.6	114
71	Optical analysis of perovskite/silicon tandem solar cells. Journal of Materials Chemistry C, 2016, 4, 5679-5689.	5.5	112
72	Light Illumination Induced Photoluminescence Enhancement and Quenching in Lead Halide Perovskite. Solar Rrl, 2017, 1, 1600001.	5.8	109

#	Article	IF	CITATIONS
73	Triggering the Passivation Effect of Potassium Doping in Mixedâ€Cation Mixedâ€Halide Perovskite by Light Illumination. Advanced Energy Materials, 2019, 9, 1901016.	19.5	109
74	TiO2 sol–gel blocking layers for dye-sensitized solar cells. Comptes Rendus Chimie, 2006, 9, 622-626.	0.5	104
75	Enhanced open-circuit voltage of p-type DSC with highly crystalline NiO nanoparticles. Chemical Communications, 2011, 47, 4808.	4.1	104
76	Effect of the Microstructure of the Functional Layers on the Efficiency of Perovskite Solar Cells. Advanced Materials, 2017, 29, 1601715.	21.0	104
77	Role of Anion Vacancies in Nitrogen-Stabilized Zirconia. Journal of the American Ceramic Society, 1993, 76, 683-688.	3.8	103
78	Thin Films of Dendritic Anatase Titania Nanowires Enable Effective Holeâ€Blocking and Efficient Lightâ€Harvesting for Highâ€Performance Mesoscopic Perovskite Solar Cells. Advanced Functional Materials, 2015, 25, 3264-3272.	14.9	101
79	Stability Comparison of Perovskite Solar Cells Based on Zinc Oxide and Titania on Polymer Substrates. ChemSusChem, 2016, 9, 687-695.	6.8	101
80	Unraveling the Morphology of High Efficiency Polymer Solar Cells Based on the Donor Polymer PBDTTT‣FT. Advanced Energy Materials, 2015, 5, 1401259.	19.5	100
81	Low-Temperature TiO _{<i>x</i>} Compact Layer for Planar Heterojunction Perovskite Solar Cells. ACS Applied Materials & Interfaces, 2016, 8, 11076-11083.	8.0	100
82	Silver Bismuth Sulfoiodide Solar Cells: Tuning Optoelectronic Properties by Sulfide Modification for Enhanced Photovoltaic Performance. Advanced Energy Materials, 2019, 9, 1803396.	19.5	100
83	Improved photocurrents for p-type dye-sensitized solar cells using nano-structured nickel(ii) oxide microballs. Energy and Environmental Science, 2012, 5, 8896.	30.8	99
84	Spiro-thiophene derivatives as hole-transport materials for perovskite solar cells. Journal of Materials Chemistry A, 2015, 3, 12139-12144.	10.3	96
85	Resistance of alkali-activated slag concrete to alkali–aggregate reaction. Cement and Concrete Research, 2001, 31, 331-334.	11.0	93
86	Remarkable photocurrent of p-type dye-sensitized solar cell achieved by size controlled CuGaO ₂ nanoplates. Journal of Materials Chemistry A, 2014, 2, 2968-2976.	10.3	93
87	4-tert-Butylpyridine Free Hole Transport Materials for Efficient Perovskite Solar Cells: A New Strategy to Enhance the Environmental and Thermal Stability. ACS Energy Letters, 2018, 3, 1677-1682.	17.4	92
88	NiO nanosheets as efficient top hole transporters for carbon counter electrode based perovskite solar cells. Journal of Materials Chemistry A, 2015, 3, 24121-24127.	10.3	91
89	Inverted perovskite solar cells with high fill-factors featuring chemical bath deposited mesoporous NiO hole transporting layers. Nano Energy, 2018, 49, 163-171.	16.0	91
90	Enhancing the Optoelectronic Performance of Perovskite Solar Cells via a Textured CH ₃ NH ₃ PbI ₃ Morphology. Advanced Functional Materials, 2016, 26, 1278-1285.	14.9	90

#	Article	IF	CITATIONS
91	Low temperature processing of flexible planar perovskite solar cells with efficiency over 10%. Journal of Power Sources, 2015, 278, 325-331.	7.8	89
92	Lowâ€Cost <i>N</i> , <i>N</i> ′â€Bicarbazoleâ€Based Dopantâ€Free Holeâ€Transporting Materials for Largeâ€ Perovskite Solar Cells. Advanced Energy Materials, 2018, 8, 1800538.	Area 19.5	89
93	Efficient and stable planar all-inorganic perovskite solar cells based on high-quality CsPbBr3 films with controllable morphology. Journal of Energy Chemistry, 2020, 46, 8-15.	12.9	89
94	Modulating crystal growth of formamidinium–caesium perovskites for over 200 cm2 photovoltaic sub-modules. Nature Energy, 2022, 7, 528-536.	39.5	89
95	Print flexible solar cells. Nature, 2016, 539, 488-489.	27.8	85
96	LiTFSIâ€Free Spiroâ€OMeTADâ€Based Perovskite Solar Cells with Power Conversion Efficiencies Exceeding 19%. Advanced Energy Materials, 2019, 9, 1901519.	19.5	85
97	Phase Relationships and Related Microstructural Observations in the Caâ€Siâ€Alâ€Oâ€N System. Journal of the American Ceramic Society, 1998, 81, 1781-1788.	3.8	84
98	Aqueous dye-sensitized solar cell electrolytes based on the cobalt(<scp>ii</scp>)/(<scp>iii</scp>) tris(bipyridine) redox couple. Energy and Environmental Science, 2013, 6, 121-127.	30.8	81
99	Low-Temperature Presynthesized Crystalline Tin Oxide for Efficient Flexible Perovskite Solar Cells and Modules. ACS Applied Materials & Interfaces, 2018, 10, 14922-14929.	8.0	81
100	Hydrothermal synthesis of bismuth oxide needles. Materials Letters, 2002, 55, 46-49.	2.6	80
101	Anisotropic grain growth of Bi4Ti3O12 in molten salt fluxes. Materials Research Bulletin, 2003, 38, 567-576.	5.2	79
102	Low temperature chemically sintered nano-crystalline TiO2 electrodes for flexible dye-sensitized solar cells. Journal of Photochemistry and Photobiology A: Chemistry, 2010, 213, 30-36.	3.9	78
103	Chemical Dopant Engineering in Hole Transport Layers for Efficient Perovskite Solar Cells: Insight into the Interfacial Recombination. ACS Nano, 2018, 12, 10452-10462.	14.6	78
104	Dye-sensitized CuAlO ₂ photocathodes for tandem solar cell applications. Journal of Photonics for Energy, 2011, 1, 011103.	1.3	77
105	Four-Terminal Tandem Solar Cells Using CH ₃ NH ₃ PbBr ₃ by Spectrum Splitting. Journal of Physical Chemistry Letters, 2015, 6, 3931-3934.	4.6	77
106	Visualizing Phase Segregation in Mixedâ€Halide Perovskite Single Crystals. Angewandte Chemie - International Edition, 2019, 58, 2893-2898.	13.8	77
107	Microstructural Development of Calcium alphaâ€5iAlON Ceramics with Elongated Grains. Journal of the American Ceramic Society, 1999, 82, 421-428.	3.8	76
108	One-Pot Synthesis of Self-Stabilized Aqueous Nanoinks for Cu ₂ ZnSn(S,Se) ₄ Solar Cells. Chemistry of Materials, 2014, 26, 3573-3578.	6.7	76

#	Article	IF	CITATIONS
109	Photoluminescence and electroluminescence imaging of perovskite solar cells. Progress in Photovoltaics: Research and Applications, 2015, 23, 1697-1705.	8.1	76
110	Fatigue behavior of planar CH3NH3PbI3 perovskite solar cells revealed by light on/off diurnal cycling. Nano Energy, 2016, 27, 509-514.	16.0	76
111	Planar versus mesoscopic perovskite microstructures: The influence of CH3NH3PbI3 morphology on charge transport and recombination dynamics. Nano Energy, 2016, 22, 439-452.	16.0	76
112	Wavelength-tunable waveguides based on polycrystalline organic–inorganic perovskite microwires. Nanoscale, 2016, 8, 6258-6264.	5.6	76
113	Microstructural Characterisations of Perovskite Solar Cells – From Grains to Interfaces: Techniques, Features, and Challenges. Advanced Energy Materials, 2017, 7, 1700912.	19.5	76
114	Development of polymer–ceramic composites for improved fire resistance. Journal of Materials Processing Technology, 2004, 153-154, 401-407.	6.3	75
115	On the Origin of Hysteresis in Perovskite Solar Cells. Advanced Functional Materials, 2016, 26, 6807-6813.	14.9	74
116	Large-area perovskite solar cells with Cs _x FA _{1â^'x} PbI _{3â^'y} Br _y thin films deposited by a vapor–solid reaction method. Journal of Materials Chemistry A, 2018, 6, 21143-21148.	10.3	73
117	Improved Photovoltages for p-Type Dye-Sensitized Solar Cells Using CuCrO ₂ Nanoparticles. Journal of Physical Chemistry C, 2014, 118, 16375-16379.	3.1	72
118	Pyrolysis behaviour of silicone-based ceramifying composites. Materials Science & Engineering A: Structural Materials: Properties, Microstructure and Processing, 2006, 425, 7-14.	5.6	70
119	Synthesis and Characterization of CuAlO ₂ and AgAlO ₂ Delafossite Oxides through Low-Temperature Hydrothermal Methods. Inorganic Chemistry, 2014, 53, 4106-4116.	4.0	70
120	How reliable are efficiency measurements of perovskite solar cells? The first inter-comparison, between two accredited and eight non-accredited laboratories. Journal of Materials Chemistry A, 2017, 5, 22542-22558.	10.3	70
121	Thin Films of Tin Oxide Nanosheets Used as the Electron Transporting Layer for Improved Performance and Ambient Stability of Perovskite Photovoltaics. Solar Rrl, 2017, 1, 1700117.	5.8	69
122	Formation of strong ceramified ash from silicone-based compositions. Journal of Materials Science, 2005, 40, 5741-5749.	3.7	68
123	Enhanced Performance of pâ€Type Dyeâ€5ensitized Solar Cells Based on Ultrasmall Mgâ€Doped CuCrO ₂ Nanocrystals. ChemSusChem, 2013, 6, 1432-1437.	6.8	68
124	Reversible Structural Swell–Shrink and Recoverable Optical Properties in Hybrid Inorganic–Organic Perovskite. ACS Nano, 2016, 10, 7031-7038.	14.6	68
125	Alkali Cation Doping for Improving the Structural Stability of 2D Perovskite in 3D/2D PSCs. Nano Letters, 2020, 20, 1240-1251.	9.1	68
126	Cold isostatic pressing technique for producing highly efficient flexible dyeâ€sensitised solar cells on plastic substrates. Progress in Photovoltaics: Research and Applications, 2012, 20, 321-332.	8.1	67

#	Article	IF	CITATIONS
127	Zinc Porphyrins with a Pyridineâ€Ringâ€Anchoring Group for Dyeâ€Sensitized Solar Cells. Chemistry - an Asian Journal, 2013, 8, 956-962.	3.3	67
128	Efficient mesoscopic perovskite solar cells based on the CH ₃ NH ₃ PbI ₂ Br light absorber. Journal of Materials Chemistry A, 2015, 3, 9116-9122.	10.3	67
129	Light induced degradation in mixed-halide perovskites. Journal of Materials Chemistry C, 2019, 7, 9326-9334.	5.5	67
130	Aluminum-Containing Nilrogen Melilite Phases. Journal of the American Ceramic Society, 1994, 77, 143-148.	3.8	66
131	Organic Sensitizers with Pyridine Ring Anchoring Group for p-Type Dye-Sensitized Solar Cells. Journal of Physical Chemistry C, 2014, 118, 16433-16440.	3.1	66
132	Dipole-field-assisted charge extraction in metal-perovskite-metal back-contact solar cells. Nature Communications, 2017, 8, 613.	12.8	66
133	Zn-doped TiO2 electrodes in dye-sensitized solar cells for enhanced photocurrent. Journal of Materials Chemistry, 2012, 22, 17128.	6.7	65
134	Formation of anatase TiO2 by microwave processing. Solar Energy Materials and Solar Cells, 2004, 84, 135-143.	6.2	64
135	D–π–A structured porphyrins for efficient dye-sensitized solar cells. Journal of Materials Chemistry A, 2013, 1, 10008.	10.3	64
136	A printable graphene enhanced composite counter electrode for flexible dye-sensitized solar cells. Nano Energy, 2013, 2, 235-240.	16.0	64
137	Fine Tuning of Fluorene-Based Dye Structures for High-Efficiency <i>p</i> -Type Dye-Sensitized Solar Cells. ACS Applied Materials & Interfaces, 2014, 6, 10614-10622.	8.0	64
138	Directing nucleation and growth kinetics in solution-processed hybrid perovskite thin-films. Science China Materials, 2017, 60, 617-628.	6.3	64
139	Study on gelcasting and properties of recrystallized silicon carbide. Ceramics International, 2002, 28, 369-376.	4.8	63
140	Effects of dispersants and soluble counter-ions on aqueous dispersibility of nano-sized zirconia powder. Ceramics International, 2004, 30, 219-224.	4.8	63
141	Nitrogen-Containing Tetragonal Zirconia. Journal of the American Ceramic Society, 1991, 74, 1135-1138.	3.8	62
142	Erosion of alumina ceramics by air- and water-suspended garnet particles. Wear, 2000, 240, 40-51.	3.1	62
143	Preferential orientation of muscovite in ceramifiable silicone composites. Materials Science & Engineering A: Structural Materials: Properties, Microstructure and Processing, 2005, 398, 180-187.	5.6	62
144	Investigation of the ceramifying process of modified silicone–silicate compositions. Journal of Materials Science, 2007, 42, 6046-6055.	3.7	62

#	Article	IF	CITATIONS
145	Saturation ratio of poly(ethylene oxide) to silicate in melt intercalated nanocomposites. European Polymer Journal, 2003, 39, 1917-1924.	5.4	61
146	Increased nanopore filling: Effect on monolithic all-solid-state dye-sensitized solar cells. Applied Physics Letters, 2007, 90, 213510.	3.3	61
147	Efficient and stable mixed perovskite solar cells using P3HT as a hole transporting layer. Journal of Materials Chemistry C, 2018, 6, 5733-5737.	5.5	61
148	Fabrication of textured bismuth titanate by templated grain growth using aqueous tape casting. Journal of the European Ceramic Society, 2003, 23, 2163-2169.	5.7	60
149	Modification of mesoporous TiO2electrodes by surface treatment with titanium(IV), indium(III) and zirconium(IV) oxide precursors: preparation, characterization and photovoltaic performance in dye-sensitized nanocrystalline solar cells. Nanotechnology, 2007, 18, 125608.	2.6	60
150	Role of Pores in the Carbothermal Reduction of Carbonâ´`Silica Nanocomposites into Silicon Carbide Nanostructures. Journal of Physical Chemistry C, 2007, 111, 636-641.	3.1	60
151	Sensitization of nickel oxide: improved carrier lifetime and charge collection by tuning nanoscale crystallinity. Chemical Communications, 2012, 48, 9885.	4.1	60
152	Synthesis and characterization of perylene–bithiophene–triphenylamine triads: studies on the effect of alkyl-substitution in p-type NiO based photocathodes. Journal of Materials Chemistry, 2012, 22, 7366.	6.7	60
153	A comparison of microwave and conventional heat treatments of nanocrystalline TiO2. Solar Energy Materials and Solar Cells, 2007, 91, 6-16.	6.2	59
154	Low-cost porous Cu2ZnSnSe4 film remarkably superior to noble Pt as counter electrode in quantum dot-sensitized solar cell system. Journal of Power Sources, 2013, 226, 359-362.	7.8	57
155	Probing Molecular and Crystalline Orientation in Solutionâ€Processed Perovskite Solar Cells. Advanced Functional Materials, 2015, 25, 5529-5536.	14.9	57
156	Highâ€ŧhroughput method to deposit continuous composition spread Sb ₂ (Se _x S _{1Ââ^`Âx}) ₃ thin film for photovoltaic application. Progress in Photovoltaics: Research and Applications, 2018, 26, 281-290.	8.1	57
157	Two-step sequential blade-coating of high quality perovskite layers for efficient solar cells and modules. Journal of Materials Chemistry A, 2020, 8, 8447-8454.	10.3	57
158	Stacking n-type layers: Effective route towards stable, efficient and hysteresis-free planar perovskite solar cells. Nano Energy, 2018, 44, 34-42.	16.0	56
159	Nanocomposites of poly(methyl methacrylate) and organically modified layered silicates by melt intercalation. Journal of Applied Polymer Science, 2004, 92, 2101-2115.	2.6	55
160	Controlling Interfacial Recombination in Aqueous Dyeâ€ 5 ensitized Solar Cells by Octadecyltrichlorosilane Surface Treatment. Angewandte Chemie - International Edition, 2014, 53, 6933-6937.	13.8	55
161	Spray deposition of water-soluble multiwall carbon nanotube and Cu2ZnSnSe4 nanoparticle composites as highly efficient counter electrodes in a quantum dot-sensitized solar cell system. Nanoscale, 2013, 5, 6992.	5.6	54
162	Highly efficient light harvesting ruthenium sensitizers for dye-sensitized solar cells featuring triphenylamine donor antennas. Journal of Materials Chemistry A, 2014, 2, 4945-4953.	10.3	54

#	Article	IF	CITATIONS
163	Controlled Growth of Monocrystalline Organoâ€Lead Halide Perovskite and Its Application in Photonic Devices. Angewandte Chemie - International Edition, 2017, 56, 12486-12491.	13.8	54
164	An optical fibre-based sensor for the detection of gaseous ammonia with methylammonium lead halide perovskite. Journal of Materials Chemistry C, 2018, 6, 6988-6995.	5.5	54
165	High-capacity optical long data memory based on enhanced Young's modulus in nanoplasmonic hybrid glass composites. Nature Communications, 2018, 9, 1183.	12.8	54
166	Thermal Stability of Calcium α-sialon Ceramics. Journal of the European Ceramic Society, 1998, 18, 417-427.	5.7	53
167	Bi4Ti3O12 nanoparticles prepared by hydrothermal synthesis. Journal of the European Ceramic Society, 2003, 23, 161-166.	5.7	53
168	Sulfurization induced surface constitution and its correlation to the performance of solution-processed Cu2ZnSn(S,Se)4 solar cells. Scientific Reports, 2014, 4, 6288.	3.3	53
169	Solid-state Ru-dye solar cells using polypyrrole as a hole conductor. Journal Physics D: Applied Physics, 2004, 37, 13-20.	2.8	52
170	Solventâ€Mediated Dimension Tuning of Semiconducting Oxide Nanostructures as Efficient Charge Extraction Thin Films for Perovskite Solar Cells with Efficiency Exceeding 16%. Advanced Energy Materials, 2016, 6, 1502027.	19.5	52
171	Dynamic Antisolvent Engineering for Spin Coating of 10 × 10 cm ² Perovskite Solar M Approaching 18%. Solar Rrl, 2020, 4, 1900263.	19dule	52
172	Dye-sensitized nanocrystalline solar cells incorporating ethylmethylimidazolium-based ionic liquid electrolytes. Comptes Rendus Chimie, 2006, 9, 617-621.	0.5	51
173	Translucent α‧ialon Ceramics by Hot Pressing. Journal of the American Ceramic Society, 2004, 87, 730-732.	3.8	50
174	Synthesis and thermal behavior of inorganic-organic hybrid geopolymer composites. Journal of Applied Polymer Science, 2005, 96, 112-121.	2.6	50
175	A design for monolithic all-solid-state dye-sensitized solar cells with a platinized carbon counterelectrode. Applied Physics Letters, 2009, 94, 103102.	3.3	50
176	Rutile TiO2 microspheres with exposed nano-acicular single crystals for dye-sensitized solar cells. Nano Research, 2011, 4, 938-947.	10.4	50
177	Efficient p-type dye-sensitized solar cells based on disulfide/thiolate electrolytes. Nanoscale, 2013, 5, 7963.	5.6	50
178	Boosting the Photocurrent Density of p-Type Solar Cells Based on Organometal Halide Perovskite-Sensitized Mesoporous NiO Photocathodes. ACS Applied Materials & Interfaces, 2014, 6, 12609-12617.	8.0	50
179	Sol–gel derived composites from poly(silicic acid) and 2-hydroxyethylmethacrylate: thermal, physical and morphological properties. Polymer, 2002, 43, 4627-4638.	3.8	49
180	Efficient Perovskite Solar Cells Employing Inorganic Interlayers. ChemNanoMat, 2016, 2, 182-188.	2.8	49

#	Article	IF	CITATIONS
181	Improved air stability of perovskite hybrid solar cells via blending poly(dimethylsiloxane)–urea copolymers. Journal of Materials Chemistry A, 2017, 5, 5486-5494.	10.3	49
182	Design and synthesis of dopant-free organic hole-transport materials for perovskite solar cells. Chemical Communications, 2018, 54, 9571-9574.	4.1	49
183	Preparation and grain boundary devitrification of samarium α-sialon ceramics. Journal of the European Ceramic Society, 1994, 14, 13-21.	5.7	48
184	Gelcasting of silicon carbide based on gelation of sodium alginate. Ceramics International, 2002, 28, 865-871.	4.8	48
185	Lanthanum modified bismuth titanate prepared by a hydrolysis method. Journal of Materials Chemistry, 2004, 14, 3566.	6.7	48
186	Modulated Charge Injection in p-Type Dye-Sensitized Solar Cells Using Fluorene-Based Light Absorbers. ACS Applied Materials & Interfaces, 2014, 6, 3448-3454.	8.0	48
187	Spray deposition of AgBiS ₂ and Cu ₃ BiS ₃ thin films for photovoltaic applications. Journal of Materials Chemistry C, 2018, 6, 2483-2494.	5.5	48
188	Surface modification <i>via</i> self-assembling large cations for improved performance and modulated hysteresis of perovskite solar cells. Journal of Materials Chemistry A, 2019, 7, 6793-6800.	10.3	48
189	Printing strategies for scaling-up perovskite solar cells. National Science Review, 2021, 8, nwab075.	9.5	48
190	Wearable and sensitive heart-rate detectors based on PbS quantum dot and multiwalled carbon nanotube blend film. Applied Physics Letters, 2014, 105, .	3.3	47
191	Slow Response of Carrier Dynamics in Perovskite Interface upon Illumination. ACS Applied Materials & Interfaces, 2018, 10, 31452-31461.	8.0	47
192	Nitrogenâ€doped tin oxide electron transport layer for stable perovskite solar cells with efficiency over 23%. , 2022, 1, 309-315.		47
193	Surface State Recombination and Passivation in Nanocrystalline TiO2 Dye-Sensitized Solar Cells. Journal of Physical Chemistry C, 2013, 117, 25118-25126.	3.1	46
194	Fatigue stability of CH3NH3PbI3 based perovskite solar cells in day/night cycling. Nano Energy, 2019, 58, 687-694.	16.0	46
195	High performance perovskite sub-module with sputtered SnO2 electron transport layer. Solar Energy, 2019, 183, 306-314.	6.1	46
196	Gelcasting of alumina ceramics in the mixed acrylamide and polyacrylamide systems. Journal of the European Ceramic Society, 2003, 23, 2273-2279.	5.7	45
197	Fabrication of efficient solar cells on plastic substrates using binder-free ball milled titania slurries. Journal of Photochemistry and Photobiology A: Chemistry, 2009, 206, 64-70.	3.9	45
198	Efficient and Stable Inverted Planar Perovskite Solar Cells Using a Triphenylamine Holeâ€Transporting Material. ChemSusChem, 2018, 11, 1467-1473.	6.8	45

#	Article	IF	CITATIONS
199	Novel porphyrin-preparation, characterization, and applications in solar energy conversion. Physical Chemistry Chemical Physics, 2016, 18, 6885-6892.	2.8	44
200	A facile deposition method for CuSCN: Exploring the influence of CuSCN on J-V hysteresis in planar perovskite solar cells. Nano Energy, 2017, 32, 310-319.	16.0	44
201	Back-contact perovskite solar cells with honeycomb-like charge collecting electrodes. Nano Energy, 2018, 50, 710-716.	16.0	44
202	Raman Spectroscopy of Formamidinium-Based Lead Halide Perovskite Single Crystals. Journal of Physical Chemistry C, 2020, 124, 2265-2272.	3.1	44
203	Structure engineering of hierarchical layered perovskite interface for efficient and stable wide bandgap photovoltaics. Nano Energy, 2020, 75, 104917.	16.0	44
204	Influence of starting material composition and carbon content on the preparation of Mg-α SiAlON powders by carbothermal reduction-nitridation. Journal of the European Ceramic Society, 2002, 22, 2989-2996.	5.7	42
205	Nanostructured ZrO2-Coated TiO2 Electrodes for Dye-Sensitised Solar Cells. Journal of Sol-Gel Science and Technology, 2004, 32, 363-366.	2.4	42
206	Charge transport in photocathodes based on the sensitization of NiO nanorods. Journal of Materials Chemistry, 2012, 22, 7005.	6.7	42
207	Graphene/titanium carbide composites prepared by sol–gel infiltration and spark plasma sintering. Ceramics International, 2016, 42, 122-131.	4.8	42
208	Moisture assisted CsPbBr3 film growth for high-efficiency, all-inorganic solar cells prepared by a multiple sequential vacuum deposition method. Materials Science in Semiconductor Processing, 2019, 98, 39-43.	4.0	42
209	Solvent Engineering of a Dopant-Free Spiro-OMeTAD Hole-Transport Layer for Centimeter-Scale Perovskite Solar Cells with High Efficiency and Thermal Stability. ACS Applied Materials & Interfaces, 2020, 12, 8260-8270.	8.0	42
210	Efficient and stable perovskite solar cells via surface passivation of an ultrathin hydrophobic organic molecular layer. Chemical Engineering Journal, 2021, 405, 126712.	12.7	42
211	Anomalous rheological behavior in chemically modified TiO2 colloidal pastes prepared for flexible dye-sensitized solar cells. Journal of Materials Chemistry, 2010, 20, 9954.	6.7	41
212	Flexible dye-sensitized solar cells containing multiple dyes in discrete layers. Energy and Environmental Science, 2011, 4, 2803.	30.8	41
213	Titanium Carbide and Titanium Nitride-Based Nanocomposites as Efficient Catalysts for the Co ²⁺ /Co ³⁺ Redox Couple in Dye-Sensitized Solar Cells. Journal of Physical Chemistry C, 2014, 118, 16818-16824.	3.1	41
214	Universal defects elimination for high performance thermally evaporated CsPbBr3 perovskite solar cells. Solar Energy Materials and Solar Cells, 2020, 206, 110317.	6.2	41
215	Effect of Mesoporous TiO2 Bead Diameter in Working Electrodes on the Efficiency of Dye-Sensitized Solar Cells. ChemSusChem, 2011, 4, 1498-1503.	6.8	40
216	Selective laser sintering of TiO ₂ nanoparticle film on plastic conductive substrate for highly efficient flexible dye-sensitized solar cell application. Journal of Materials Chemistry A, 2014, 2, 4566-4573.	10.3	40

#	Article	IF	CITATIONS
217	Preferred orientation in hot-pressed Ca ?-SiAlON ceramics. Journal of Materials Science Letters, 1996, 15, 1447-1449.	0.5	39
218	Carbon film electrode based square-centimeter scale planar perovskite solar cells exceeding 17% efficiency. Materials Science in Semiconductor Processing, 2020, 107, 104809.	4.0	39
219	Low-temperature sintering of Bi4Ti3O12 derived from a co-precipitation method. Materials Letters, 2002, 56, 910-914.	2.6	38
220	A facile approach to alleviate photochemical degradation in high efficiency polymer solar cells. Journal of Materials Chemistry A, 2015, 3, 16313-16319.	10.3	38
221	Influence of Fullerene Acceptor on the Performance, Microstructure, and Photophysics of Low Bandgap Polymer Solar Cells. Advanced Energy Materials, 2017, 7, 1602197.	19.5	38
222	TiO ₂ Nanorods: A Facile Size- and Shape-Tunable Synthesis and Effective Improvement of Charge Collection Kinetics for Dye-Sensitized Solar Cells. ACS Applied Materials & Interfaces, 2014, 6, 9698-9704.	8.0	37
223	Preparation of p-type AgCrO2 nanocrystals through low-temperature hydrothermal method and the potential application in p-type dye-sensitized solar cell. Journal of Alloys and Compounds, 2015, 642, 104-110.	5.5	37
224	Stabilizing High Efficiency Perovskite Solar Cells with 3D-2D Heterostructures. Joule, 2020, 4, 975-979.	24.0	37
225	Synthesis of nanostructured silicon carbide spheres from mesoporous C–SiO ₂ nanocomposites. Chemical Communications, 2010, 46, 303-305.	4.1	36
226	In-Depth Understanding of the Morphology–Performance Relationship in Polymer Solar Cells. ACS Applied Materials & Interfaces, 2015, 7, 14026-14034.	8.0	36
227	Impact of microstructure on the electron–hole interaction in lead halide perovskites. Energy and Environmental Science, 2017, 10, 1358-1366.	30.8	36
228	Influence of α-alumina seed on the morphology of grain growth in alumina ceramics from Bayer aluminum hydroxide. Materials Letters, 2003, 57, 2501-2508.	2.6	35
229	Microstructural Tailoring and Characterization of a Calcium αâ€SiAlON Composition. Journal of the American Ceramic Society, 2002, 85, 812-818.	3.8	35
230	Pyrene-conjugated porphyrins for efficient mesoscopic solar cells: the role of the spacer. Journal of Materials Chemistry A, 2014, 2, 17495-17501.	10.3	35
231	Thiophene-Functionalized Porphyrins: Synthesis, Photophysical Properties, and Photovoltaic Performance in Dye-Sensitized Solar Cells. Journal of Physical Chemistry C, 2015, 119, 5265-5273.	3.1	35
232	Photovoltaic performance and the energy landscape of CH ₃ NH ₃ PbI ₃ . Physical Chemistry Chemical Physics, 2015, 17, 22604-22615.	2.8	35
233	Robust transparent superamphiphobic coatings on non-fabric flat substrates with inorganic adhesive titania bonded silica. Journal of Materials Chemistry A, 2017, 5, 8352-8359.	10.3	35
234	An efficient, flexible perovskite solar module exceeding 8% prepared with an ultrafast PbI2 deposition rate. Scientific Reports, 2018, 8, 442.	3.3	35

#	Article	IF	CITATIONS
235	Self-augmented ion blocking of sandwiched 2D/1D/2D electrode for solution processed high efficiency semitransparent perovskite solar cell. Nano Energy, 2020, 71, 104567.	16.0	35
236	Organic–inorganic hybrids derived from 2-hydroxyethylmethacrylate and (3-methacryloyloxypropyl)trimethoxysilane. Polymer, 2002, 43, 4123-4136.	3.8	34
237	Formation of novel mesoporous TiC microspheres through a sol–gel and carbothermal reduction process. Journal of the European Ceramic Society, 2012, 32, 3407-3414.	5.7	34
238	Microstructures and properties of Si3N4/TiN composites sintered by hot pressing and spark plasma sintering. Materials Research Bulletin, 2013, 48, 1927-1933.	5.2	34
239	Conducting polymer and titanium carbide-based nanocomposites as efficient counter electrodes for dye-sensitized solar cells. Electrochimica Acta, 2013, 105, 275-281.	5.2	34
240	Potassiumâ€Doped Zinc Oxide as Photocathode Material in Dyeâ€Sensitized Solar Cells. ChemSusChem, 2013, 6, 622-629.	6.8	34
241	Titania nanobundle networks as dye-sensitized solar cell photoanodes. Nanoscale, 2014, 6, 3704-3711.	5.6	34
242	Al ₂ O ₃ Underlayer Prepared by Atomic Layer Deposition for Efficient Perovskite Solar Cells. ChemSusChem, 2017, 10, 3810-3817.	6.8	34
243	Generalized Water-Processed Metal Chalcogenide Complexes: Synthesis and Applications. Chemistry of Materials, 2015, 27, 8048-8057.	6.7	33
244	Musselâ€Directed Synthesis of Nitrogenâ€Doped Anatase TiO ₂ . Angewandte Chemie - International Edition, 2016, 55, 3031-3035.	13.8	33
245	Synthesis of Mg-α SiAlON powders from talc and halloysite clay minerals. Journal of the European Ceramic Society, 2000, 20, 1809-1814.	5.7	32
246	XRD analysis of formation of strontium barium niobate phase. Materials Letters, 2002, 56, 915-920.	2.6	32
247	Al-Containing Porous Titanium Dioxide Networks:Â Solâ~'Gel Synthesis within Agarose Gel Template and Photocatalytic Activity. Chemistry of Materials, 2006, 18, 5835-5839.	6.7	32
248	Preparation and properties of neodymium-modified bismuth titanate ceramics. Journal of the European Ceramic Society, 2008, 28, 1641-1647.	5.7	32
249	Synthesis and Evolution of Zirconium Carbide via Sol–Gel Route: Features of Nanoparticle Oxide–Carbon Reactions. Journal of the American Ceramic Society, 2013, 96, 1099-1106.	3.8	32
250	Ultrafast Fabrication of Flexible Dye-Sensitized Solar Cells by Ultrasonic Spray-Coating Technology. Scientific Reports, 2015, 5, 14645.	3.3	32
251	Effect of Grain Cluster Size on Backâ€Contact Perovskite Solar Cells. Advanced Functional Materials, 2018, 28, 1805098.	14.9	32
252	Rationally Induced Interfacial Dipole in Planar Heterojunction Perovskite Solar Cells for Reduced <i>J</i> – <i>V</i> Hysteresis. Advanced Energy Materials, 2018, 8, 1800568.	19.5	32

#	Article	IF	CITATIONS
253	Microwave processing of TiO2 blocking layers for dye-sensitized solar cells. Journal of Sol-Gel Science and Technology, 2006, 40, 45-54.	2.4	31
254	Construction of nanostructured electrodes on flexible substrates using pre-treated building blocks. Applied Physics Letters, 2012, 100, .	3.3	31
255	4-fold photocurrent enhancement in ultrathin nanoplasmonic perovskite solar cells. Optics Express, 2015, 23, A1700.	3.4	31
256	Organized intrafibrillar mineralization, directed by a rationally designed multi-functional protein. Journal of Materials Chemistry B, 2015, 3, 4496-4502.	5.8	31
257	Isolating and quantifying the impact of domain purity on the performance of bulk heterojunction solar cells. Energy and Environmental Science, 2017, 10, 1843-1853.	30.8	31
258	Enhanced Crystallinity of Lowâ€Temperature Solutionâ€Processed SnO ₂ for Highly Reproducible Planar Perovskite Solar Cells. ChemSusChem, 2018, 11, 2898-2903.	6.8	31
259	Role of microstructure in the grinding and polishing of α-sialon ceramics. Journal of the European Ceramic Society, 2003, 23, 2351-2360.	5.7	30
260	Solution-processed Zn2SnO4 electron transporting layer for efficient planar perovskite solar cells. Materials Today Energy, 2018, 7, 260-266.	4.7	30
261	Controlling Homogenous Spherulitic Crystallization for Highâ€Efficiency Planar Perovskite Solar Cells Fabricated under Ambient Highâ€Humidity Conditions. Small, 2019, 15, e1904422.	10.0	30
262	Elongated α-sialon grains in pressureless sintered sialon ceramics. Journal of the European Ceramic Society, 1998, 18, 1053-1057.	5.7	29
263	A novel approach for preparation of dense TiC–SiC nanocomposites by sol–gel infiltration and spark plasma sintering. Journal of the European Ceramic Society, 2014, 34, 1949-1954.	5.7	29
264	Batch chemical bath deposition of large-area SnO2 film with mercaptosuccinic acid decoration for homogenized and efficient perovskite solar cells. Chemical Engineering Journal, 2021, 425, 131444.	12.7	29
265	Title is missing!. Journal of Materials Science, 1997, 32, 83-89.	3.7	28
266	Study on gelcasting of silicon nitride-bonded silicon carbide refractories. Materials Letters, 2002, 56, 895-900.	2.6	28
267	Formation of silicon nitride bonded silicon carbide by aqueous gelcasting. Materials Science & Engineering A: Structural Materials: Properties, Microstructure and Processing, 2003, 349, 20-28.	5.6	28
268	Formation and Sintering Mechanisms of Reaction Bonded Silicon Carbide-Boron Carbide Composites. Key Engineering Materials, 2007, 352, 207-212.	0.4	28
269	Sol–gel synthesis of SiC–TiO2nanoparticles for microwave processing. Nanotechnology, 2007, 18, 055708.	2.6	28
270	On the Role of the Spacer Layer in Monolithic Dye-Sensitized Solar Cells. Journal of Physical Chemistry C, 2010, 114, 2365-2369.	3.1	28

#	Article	IF	CITATIONS
271	Tailoring the conduction band of titanium oxide by doping tungsten for efficient electron injection in a sensitized photoanode. Nanoscale, 2014, 6, 3875-3880.	5.6	28
272	Optimizing semiconductor thin films with smooth surfaces and well-interconnected networks for high-performance perovskite solar cells. Journal of Materials Chemistry A, 2016, 4, 12463-12470.	10.3	28
273	Organic/inorganic self-doping controlled crystallization and electronic properties of mixed perovskite solar cells. Journal of Materials Chemistry A, 2018, 6, 6319-6326.	10.3	28
274	Improved Performance of Planar Perovskite Solar Cells Using an Amino-Terminated Multifunctional Fullerene Derivative as the Passivation Layer. ACS Applied Materials & Interfaces, 2019, 11, 27145-27152.	8.0	28
275	Long-Distance Ionic Diffusion in Cesium Lead Mixed Halide Perovskite Induced by Focused Illumination. Chemistry of Materials, 2019, 31, 9049-9056.	6.7	28
276	The impact of spiro-OMeTAD photodoping on the reversible light-induced transients of perovskite solar cells. Nano Energy, 2021, 82, 105658.	16.0	28
277	Towards an all-polymer cathode for dye sensitized photovoltaic cells. Thin Solid Films, 2010, 518, 2871-2875.	1.8	27
278	Spiky Mesoporous Anatase Titania Beads: A Metastable Ammonium Titanateâ€Mediated Synthesis. Chemistry - A European Journal, 2012, 18, 13762-13769.	3.3	27
279	A Bi-layer TiO ₂ photoanode for highly durable, flexible dye-sensitized solar cells. Journal of Materials Chemistry A, 2015, 3, 4679-4686.	10.3	27
280	Humidity controlled sol-gel Zr/TiO2 with optimized band alignment for efficient planar perovskite solar cells. Solar Energy, 2016, 139, 290-296.	6.1	27
281	Synthesis of (Ca,Mg)-α-sialon from slag by self-propagating high-temperature synthesis. Journal of Materials Chemistry, 2002, 12, 1199-1202.	6.7	26
282	Dâ~'π–A Porphyrin Sensitizers with Ï€-Extended Conjugation for Mesoscopic Solar Cells. Journal of Physical Chemistry C, 2014, 118, 14739-14748.	3.1	26
283	Oriented Attachment as the Mechanism for Microstructure Evolution in Chloride-Derived Hybrid Perovskite Thin Films. ACS Applied Materials & Interfaces, 2019, 11, 39930-39939.	8.0	26
284	Hollow Beads Composed of Nanosize Ca α‣iAlON Grains. Journal of the American Ceramic Society, 2000, 83, 995-997.	3.8	25
285	Cobalt Polypyridyl Complexes as Transparent Solutionâ€Processable Solid‣tate Charge Transport Materials. Advanced Energy Materials, 2016, 6, 1600874.	19.5	25
286	Influence of sol-gel derived ZrB 2 additions on microstructure and mechanical properties of SiBCN composites. Ceramics International, 2017, 43, 4372-4378.	4.8	25
287	Sequentially Reinforced Additive Coating for Transparent and Durable Superhydrophobic Glass. Langmuir, 2018, 34, 11316-11324.	3.5	25
288	Effects of molecular weight and clay organo-ions on the melt intercalation of poly(ethylene oxide) into layered silicates. Polymer Engineering and Science, 2002, 42, 2369-2382.	3.1	24

#	Article	IF	CITATIONS
289	Al-doped TiO2 Photoanode for Dye-Sensitized Solar Cells. Australian Journal of Chemistry, 2011, 64, 820.	0.9	24
290	Near Field Enhanced Photocurrent Generation in P-type Dye-Sensitized Solar Cells. Scientific Reports, 2014, 4, 3961.	3.3	24
291	Impact of Fullerene Mixing Behavior on the Microstructure, Photophysics, and Device Performance of Polymer/Fullerene Solar Cells. ACS Applied Materials & Interfaces, 2016, 8, 29608-29618.	8.0	24
292	Thermal ablation behavior of SiBCN-Zr composites prepared by reactive spark plasma sintering. Ceramics International, 2017, 43, 7978-7983.	4.8	24
293	Elimination of Surface Spallation of Alumina Green Bodies Prepared by Acrylamideâ€Based Gelcasting via Poly(vinylpyrrolidone). Journal of the American Ceramic Society, 2003, 86, 266-272.	3.8	23
294	The Effect of the Scattering Layer in Dyeâ€Sensitized Solar Cells Employing a Cobaltâ€Based Aqueous Gel Electrolyte. ChemSusChem, 2015, 8, 3704-3711.	6.8	23
295	Optical Probe Ion and Carrier Dynamics at the CH ₃ NH ₃ PbI ₃ Interface with Electron and Hole Transport Materials. Advanced Materials Interfaces, 2016, 3, 1600467.	3.7	23
296	Integrated planar and bulk dual heterojunctions capable of efficient electron and hole extraction for perovskite solar cells with >17% efficiency. Nano Energy, 2017, 32, 187-194.	16.0	23
297	Solvent-Mediated Intragranular-Coarsening of CH ₃ NH ₃ Pbl ₃ Thin Films toward High-Performance Perovskite Photovoltaics. ACS Applied Materials & Interfaces, 2017, 9, 31959-31967.	8.0	23
298	Influence of phase transition on stability of perovskite solar cells under thermal cycling conditions. Solar Energy, 2019, 188, 312-317.	6.1	23
299	A perovskite/silicon hybrid system with a solar-to-electric power conversion efficiency of 25.5%. Journal of Materials Chemistry A, 2019, 7, 26479-26489.	10.3	23
300	Formamidinium-Based Perovskite Solar Cells with Enhanced Moisture Stability and Performance via Confined Pressure Annealing. Journal of Physical Chemistry C, 2020, 124, 12249-12258.	3.1	23
301	Improvement of the Zirconia shell in nanostructured titania core–shell working electrodes for dye-sensitized solar cells. Materials Letters, 2005, 59, 1893-1896.	2.6	22
302	Exploring Feasibility of Multicolored CdTe Quantum Dots for In Vitro and In Vivo Fluorescent Imaging. Journal of Nanoscience and Nanotechnology, 2008, 8, 1174-1177.	0.9	22
303	Facile Synthesis, Growth Mechanism, and UVâ^'Vis Spectroscopy of Novel Urchin-like TiO ₂ /TiB ₂ Heterostructures. Crystal Growth and Design, 2009, 9, 4017-4022.	3.0	22
304	ZIFâ€11/Polybenzimidazole composite membrane with improved hydrogen separation performance. Journal of Applied Polymer Science, 2014, 131, .	2.6	22
305	Influence of microstructure on the erosive wear behaviour of Ca α-sialon materials. Journal of the European Ceramic Society, 2001, 21, 2435-2445.	5.7	21
306	Investigation of thermal and fire performance of novel hybrid geopolymer composites. Journal of Materials Science, 2004, 39, 4721-4726.	3.7	21

#	Article	IF	CITATIONS
307	Effect of V2O5 on sintering behaviour, microstructure and dielectric properties of textured Sr0.4Ba0.6Nb2O6 ceramics. Journal of the European Ceramic Society, 2005, 25, 957-962.	5.7	21
308	Modification of ZrB ₂ powders by a sol–gel ZrC precursor—A new approach for ultra high temperature ceramic composites. Journal of Asian Ceramic Societies, 2013, 1, 77-85.	2.3	21
309	Quasi-Solid-State Dye-Sensitized Solar Cells on Plastic Substrates. Journal of Physical Chemistry C, 2014, 118, 16366-16374.	3.1	21
310	Tailoring carbon nanotube/matrix interface to optimize mechanical properties of multiscale composites. Carbon, 2014, 69, 621-625.	10.3	21
311	Spectral dependence of direct and trap-mediated recombination processes in lead halide perovskites using time resolved microwave conductivity. Physical Chemistry Chemical Physics, 2016, 18, 12043-12049.	2.8	21
312	Room-temperature synthesized SnO ₂ electron transport layers for efficient perovskite solar cells. RSC Advances, 2019, 9, 9946-9950.	3.6	21
313	Decomposition of Sm α-SiAlON phases during post-sintering heat treatment. Journal of the European Ceramic Society, 1996, 16, 1001-1008.	5.7	20
314	Phase formation and microstructural evolution of Ca α-sialon using different Si 3 N 4 starting powders. Journal of the European Ceramic Society, 2000, 20, 1803-1808.	5.7	20
315	Scratch Damage in Ceramics: Role of Microstructure. Journal of the American Ceramic Society, 2003, 86, 141-148.	3.8	20
316	Fabrication and Evaluation of Ca-α SiAlON Nano Ceramics. Key Engineering Materials, 2003, 237, 105-110.	0.4	20
317	Selfâ€Propagating Highâ€Temperature Synthesis of αâ€SiAlON Doped by RE (RE=Eu,Pr,Ce) and Codoped by RE and Yttrium. Journal of the American Ceramic Society, 2004, 87, 703-705.	3.8	20
318	Characterization of nanostructured core-shell working electrodes for application in dye-sensitized solar cells. Surface and Coatings Technology, 2005, 198, 118-122.	4.8	20
319	Fluorene functionalized porphyrins as broadband absorbers for TiO ₂ nanocrystalline solar cells. Journal of Materials Chemistry A, 2014, 2, 13667.	10.3	20
320	Catalytic Activity and Impedance Behavior of Screenâ€Printed Nickel Oxide as Efficient Water Oxidation Catalysts. ChemSusChem, 2015, 8, 4266-4274.	6.8	20
321	Fabrication of Efficient and Stable Perovskite Solar Cells in Highâ€Humidity Environment through Traceâ€Đoping of Largeâ€5ized Cations. ChemSusChem, 2019, 12, 2385-2392.	6.8	20
322	A pressure-assisted annealing method for high quality CsPbBr ₃ film deposited by sequential thermal evaporation. RSC Advances, 2020, 10, 8905-8909.	3.6	20
323	Ink Engineering for Blade Coating FA-Dominated Perovskites in Ambient Air for Efficient Solar Cells and Modules. ACS Applied Materials & Interfaces, 2021, 13, 18724-18732.	8.0	20
324	Pressureless sintering and phase relationship of samarium α-sialons. Journal of the European Ceramic Society, 1994, 14, 343-349.	5.7	19

#	Article	IF	CITATIONS
325	The development of microstructure in silicon nitride-bonded silicon carbide. Journal of the European Ceramic Society, 1995, 15, 415-424.	5.7	19
326	Phase transformations in Sm (Î \pm + Î ²)-SiAlON ceramics during post-sintering heat treatments. Journal of the European Ceramic Society, 1995, 15, 1221-1228.	5.7	19
327	Gas-discharging reactions and their effect on the microstructures of green bodies in gelcasting of non-oxide materials. Materials Letters, 2000, 45, 51-57.	2.6	19
328	Gelcasting of ceramic suspension in acrylamide/polyethylene glycol systems. Ceramics International, 2002, 28, 859-864.	4.8	19
329	Effects of composition and thermal treatment on infrared transmission of Dy-α-sialon. Journal of the European Ceramic Society, 2004, 24, 2869-2877.	5.7	19
330	Challenges of producing TiO2 films by microwave heating. Surface and Coatings Technology, 2005, 198, 20-23.	4.8	19
331	Effect of TiO ₂ microbead pore size on the performance of DSSCs with a cobalt based electrolyte. Nanoscale, 2014, 6, 13787-13794.	5.6	19
332	Influence of sol–gel derived ZrO2 and ZrC additions on microstructure and properties of ZrB2 composites. Journal of the European Ceramic Society, 2014, 34, 3139-3149.	5.7	19
333	Investigation on regeneration kinetics at perovskite/oxide interface with scanning electrochemical microscopy. Journal of Materials Chemistry A, 2015, 3, 9216-9222.	10.3	19
334	Alleviate the J–V hysteresis of carbon-based perovskite solar cells via introducing additional methylammonium chloride into MAPbI3 precursor. RSC Advances, 2018, 8, 35157-35161.	3.6	19
335	Balancing Charge Extraction for Efficient Backâ€Contact Perovskite Solar Cells by Using an Embedded Mesoscopic Architecture. Advanced Energy Materials, 2021, 11, 2100053.	19.5	19
336	Interface passivation engineering for hybrid perovskite solar cells. Materials Reports Energy, 2021, 1, 100060.	3.2	19
337	Optical properties of SPS-ed Y- and (Dy,Y)-Â-sialon ceramics. Journal of Materials Science, 2004, 39, 6257-6262.	3.7	18
338	One-step microwave calcination of ZrO2-coated TiO2 electrodes for use in dye-sensitized solar cells. Comptes Rendus Chimie, 2006, 9, 713-716.	0.5	18
339	Synthesis of Mesoporous Carbonâ€Bonded <scp>TiC/SiC</scp> Composites by Direct Carbothermal Reduction of Sol–Gel Derived Monolithic Precursor. Journal of the American Ceramic Society, 2011, 94, 4025-4031.	3.8	18
340	Effects of the electric current on conductive Si3N4/TiN composites in spark plasma sintering. Journal of Alloys and Compounds, 2013, 547, 51-58.	5.5	18
341	Enhanced performance of p-type dye sensitized solar cells based on mesoporous Ni _{1â^'x} Mg _x O ternary oxide films. RSC Advances, 2014, 4, 60670-60674.	3.6	18
342	Facile synthesis of nanoporous TiC–SiC–C composites as a novel counter-electrode for dye sensitized solar cells. Microporous and Mesoporous Materials, 2014, 190, 309-315.	4.4	18

#	Article	IF	CITATIONS
343	Photovoltaic characteristics and stability of flexible dye-sensitized solar cells on ITO/PEN substrates. RSC Advances, 2014, 4, 1393-1400.	3.6	18
344	Molecular Engineering of Organic Dyes with a Holeâ€Extending Donor Tail for Efficient Allâ€Solidâ€State Dyeâ€Sensitized Solar Cells. ChemSusChem, 2015, 8, 2529-2536.	6.8	18
345	Parameters responsible for the degradation of CH 3 NH 3 PbI 3 -based solar cells on polymer substrates. Nano Energy, 2016, 22, 211-222.	16.0	18
346	Suppressed hysteresis and enhanced performance of triple cation perovskite solar cell with chlorine incorporation. Journal of Materials Chemistry C, 2018, 6, 13157-13161.	5.5	18
347	Groups-dependent phosphines as the organic redox for point defects elimination in hybrid perovskite solar cells. Journal of Energy Chemistry, 2021, 54, 23-29.	12.9	18
348	Microstructural features of the $\hat{I}\pm$ to \hat{I}^2 -SiAlON phase transformation. Journal of the European Ceramic Society, 1996, 16, 529-534.	5.7	17
349	Erosion Response of Highly Anisotropic Silicon Nitride. Journal of the American Ceramic Society, 2005, 88, 114-120.	3.8	17
350	Hot Forging of a Textured alpha-Sialon Ceramic. Journal of the American Ceramic Society, 2006, 89, 478-483.	3.8	17
351	Polypyridyl Iron Complex as a Hole-Transporting Material for Formamidinium Lead Bromide Perovskite Solar Cells. ACS Energy Letters, 2017, 2, 1855-1859.	17.4	17
352	Device preâ€conditioning and steadyâ€state temperature dependence of CH ₃ NH ₃ Pbl ₃ perovskite solar cells. Progress in Photovoltaics: Research and Applications, 2017, 25, 533-544.	8.1	17
353	Honeycomb-shaped charge collecting electrodes for dipole-assisted back-contact perovskite solar cells. Nano Energy, 2020, 67, 104223.	16.0	17
354	Differentiated Functions of Potassium Interface Passivation and Doping on Charge-Carrier Dynamics in Perovskite Solar Cells. Journal of Physical Chemistry Letters, 2022, 13, 3188-3196.	4.6	17
355	Gelcasting of alumina ceramic components in nontoxic Na-alginate–CalO3–PVP systems. Materials & Design, 2005, 26, 291-296.	5.1	16
356	Sliding wear behaviour of Ca α-sialon ceramics at 600°C in air. Wear, 2006, 260, 1356-1360.	3.1	16
357	Preparation of sialon–transition metal silicide composites. Journal of the European Ceramic Society, 2006, 26, 193-199.	5.7	16
358	Mesoporous titania beads for flexible dye-sensitized solar cells. Journal of Materials Chemistry C, 2014, 2, 1284-1289.	5.5	16
359	A bio-process inspired synthesis of vaterite (CaCO ₃), directed by a rationally designed multifunctional protein, ChiCaSifi. Journal of Materials Chemistry B, 2015, 3, 5951-5956.	5.8	16
360	Molecular Engineering of Zincâ€Porphyrin Sensitisers for pâ€Type Dye‧ensitised Solar Cells. ChemPlusChem, 2018, 83, 711-720.	2.8	16

#	Article	IF	CITATIONS
361	Toward Commercialization of Efficient and Stable Perovskite Solar Modules. Solar Rrl, 2022, 6, 2100600.	5.8	16
362	Lead contamination analysis of perovskite modules under simulated working conditions. Solar Energy, 2021, 226, 85-91.	6.1	16
363	Self-Enhancement of Efficiency and Self-Attenuation of Hysteretic Behavior of Perovskite Solar Cells with Aging. Journal of Physical Chemistry Letters, 2022, 13, 2792-2799.	4.6	16
364	The solubility of aluminium in rare earth nitrogen melilite phases. Journal of the European Ceramic Society, 1995, 15, 1213-1220.	5.7	15
365	Phase relationships and microstructures of Ca and Al-rich α-sialon ceramics. Journal of the European Ceramic Society, 2000, 20, 357-366.	5.7	15
366	Microstructural design of Ca \hat{I}_{\pm} -sialon ceramics: effects of starting compositions and processing conditions. Journal of the European Ceramic Society, 2003, 23, 1531-1541.	5.7	15
367	Optical Properties of Gd–αâ€Sialon Ceramics: Effect of Carbon Contamination. Journal of the American Ceramic Society, 2005, 88, 2304-2306.	3.8	15
368	Reversible α′↔β′ transformation in preferentially oriented sialon ceramics. Journal of the European Ceramic Society, 2006, 26, 1337-1349.	5.7	15
369	Low temperature crystallization behavior of TiO2 derived from a sol–gel process. Journal of Sol-Gel Science and Technology, 2007, 42, 107-117.	2.4	15
370	Effect of seeding on formation of silicon carbide nanostructures from mesoporous silica–carbon nanocomposites. Nanotechnology, 2008, 19, 175605.	2.6	15
371	Ca-α SiAlON hollow spheres prepared by carbothermal reduction–nitridation from different SiO2 powders. Ceramics International, 2010, 36, 1553-1559.	4.8	15
372	A cyclopenta[1,2-b:5,4-b′]dithiophene–porphyrin conjugate for mesoscopic solar cells: a D–݀–D–A approach. Physical Chemistry Chemical Physics, 2014, 16, 24755-24762.	2.8	15
373	Structural characterization of lithium aluminosilicate glass and glass ceramics derived from spodumene mineral. Journal of Physics Condensed Matter, 1995, 7, 3115-3128.	1.8	14
374	Spark Plasma Sintering of Bismuth Titanate Ceramics. Journal of the American Ceramic Society, 2005, 88, 1631-1633.	3.8	14
375	Influence of Parameters of Cold Isostatic Pressing on TiO ₂ Films for Flexible Dye-Sensitized Solar Cells. International Journal of Photoenergy, 2011, 2011, 1-7.	2.5	14
376	Modifying TiO 2 surface architecture by oxygen plasma to increase dye sensitized solar cell efficiency. Thin Solid Films, 2013, 545, 521-526.	1.8	14
377	SPS densification and microstructure of ZrB2 composites derived from sol–gel ZrC coating. Journal of the European Ceramic Society, 2014, 34, 2875-2883.	5.7	14
378	Sub-100°C solution processed amorphous titania nanowire thin films for high-performance perovskite solar cells. Journal of Power Sources, 2016, 329, 17-22.	7.8	14

#	Article	IF	CITATIONS
379	Time-resolved fluorescence anisotropy study of organic lead halide perovskite. Solar Energy Materials and Solar Cells, 2016, 151, 102-112.	6.2	14
380	High efficiency solid-state dye-sensitized solar cells using a cobalt(<scp>ii</scp> / <scp>iii</scp>) redox mediator. Journal of Materials Chemistry C, 2017, 5, 4875-4883.	5.5	14
381	Rapid preparation of conductive transparent films via solution printing of graphene precursor. Thin Solid Films, 2018, 657, 24-31.	1.8	14
382	Efficient Planar Perovskite Solar Cells via a Sputtered Cathode. Solar Rrl, 2019, 3, 1900209.	5.8	14
383	Surfactant-assisted doctor-blading-printed FAPbBr3 films for efficient semitransparent perovskite solar cells. Frontiers of Optoelectronics, 2020, 13, 272-281.	3.7	14
384	"Coffee ring―controlment in spray prepared >19% efficiency Cs0.19FA0.81Pbl2.5Br0.5 perovskite solar cells. Journal of Energy Chemistry, 2022, 67, 201-208.	12.9	14
385	Preparation of fine-grained calcium ?-sialon. Journal of Materials Science Letters, 1994, 13, 1612-1615.	0.5	13
386	Sliding wear of calcium α-sialon ceramics. Wear, 2006, 260, 387-400.	3.1	13
387	Formation Process of Calcium-α SiAlON Hollow Balls Composed of Nanosized Particles by Carbothermal Reduction–Nitridation. Journal of the American Ceramic Society, 2008, 91, 860-864.	3.8	13
388	A novel carbon–PEDOT composite counter electrode for monolithic dye-sensitized solar cells. Journal Physics D: Applied Physics, 2013, 46, 024007.	2.8	13
389	Alkyl-thiophene Functionalized D-Ï€-A Porphyrins for Mesoscopic Solar Cells. Electrochimica Acta, 2015, 179, 187-196.	5.2	13
390	Improved Efficiency and Stability of Flexible Dye Sensitized Solar Cells on <scp>ITO</scp> / <scp>PEN</scp> Substrates Using an Ionic Liquid Electrolyte. Photochemistry and Photobiology, 2015, 91, 315-322.	2.5	13
391	Metal Evaporation-Induced Degradation of Fullerene Acceptors in Polymer/Fullerene Solar Cells. ACS Applied Materials & Interfaces, 2016, 8, 2247-2254.	8.0	13
392	Three-dimensional titanium oxide nanoarrays for perovskite photovoltaics: surface engineering for cascade charge extraction and beneficial surface passivation. Sustainable Energy and Fuels, 2017, 1, 1960-1967.	4.9	13
393	Numerical analysis of a hysteresis model in perovskite solar cells. Computational Materials Science, 2017, 126, 22-28.	3.0	13
394	Oxidation behavior of SiBCN-Zr composites at 1500â€Â°C prepared by reactive spark plasma sintering. Corrosion Science, 2018, 132, 293-299.	6.6	13
395	Influence of Hot Spot Heating on Stability of Large Size Perovskite Solar Module with a Power Conversion Efficiency of a ⁻¹ /414%. ACS Applied Energy Materials, 2018, 1, 3565-3570.	5.1	13
396	Multiple Roles of Cobalt Pyrazol-Pyridine Complexes in High-Performing Perovskite Solar Cells. Journal of Physical Chemistry Letters, 2019, 10, 4675-4682.	4.6	13

#	Article	IF	CITATIONS
397	Enhancing the thermal stability of the carbon-based perovskite solar cells by using a CsxFA1â^xPbBrxI3â^x light absorber. RSC Advances, 2019, 9, 11877-11881.	3.6	13
398	Direct assessment of structural order and evidence for stacking faults in layered hybrid perovskite films from X-ray scattering measurements. Journal of Materials Chemistry A, 2020, 8, 12790-12798.	10.3	13
399	Interface modification effect on the performance of CsxFA1â^'xPblyBr3â^'y perovskite solar cells fabricated by evaporation/spray-coating method. Journal of Chemical Physics, 2020, 153, 014706.	3.0	13
400	Highâ€Performance Rb–Cs _{0.14} FA _{0.86} Pb(Br _{<i>x</i>} I _{1â^'<i>x</i>}) ₃ Perovskite Solar Cells Achieved by Regulating the Halogen Exchange in Vapor–Solid Reaction Process. Solar Rrl, 2021, 5, 2100102.	5.8	13
401	Probing the Electron Beam-Induced Structural Evolution of Halide Perovskite Thin Films by Scanning Transmission Electron Microscopy. Journal of Physical Chemistry C, 2021, 125, 10786-10794.	3.1	13
402	Radical doped hole transporting material for high-efficiency and thermostable perovskite solar cells. Journal of Materials Chemistry A, 2022, 10, 10604-10613.	10.3	13
403	NMR Investigation of the Structure of Aluminum-Containing Nitrogen Melilite (M'ss). Chemistry of Materials, 1995, 7, 982-988.	6.7	12
404	Grain Growth of alpha-SiAlON in the Calcium-Doped System. Journal of the American Ceramic Society, 2002, 85, 2545-2549.	3.8	12
405	Sequential and Simultaneous Melt Intercalation of Poly(ethylene oxide) and Poly(methyl) Tj ETQq1 1 0.784314 rgE	8T /Overloo 4.8	ck_10 Tf 50
406	Enhancing the performance and stability of carbon-based perovskite solar cells by the cold isostatic pressing method. RSC Advances, 2017, 7, 48958-48961.	3.6	12
407	Improving the crystal growth of a Cs0.24FA0.76PbI3ⰒxBrx perovskite in a vapor–solid reaction process using strontium iodide. Sustainable Energy and Fuels, 2020, 4, 2491-2496.	4.9	12
408	Intermediate phase-enhanced Ostwald ripening for the elimination of phase segregation in efficient inorganic CsPbIBr2 perovskite solar cells. Science China Materials, 2021, 64, 2655-2666.	6.3	12
409	A universal tactic of using Lewis-base polymer-CNTs composites as additives for high performance cm2-sized and flexible perovskite solar cells. Science China Chemistry, 2021, 64, 281-292.	8.2	12
410	Bromide complimented methylammonium-free wide bandgap perovskite solar modules with high efficiency and stability. Chemical Engineering Journal, 2022, 445, 136626.	12.7	12
411	Effect of additives on microstructure of Ca α-sialon. Materials Letters, 2001, 47, 281-285.	2.6	11
412	Formation behavior, microstructure and mechanical properties of multi-cation α-sialons containing calcium and neodymium. Journal of the European Ceramic Society, 2001, 21, 1273-1278.	5.7	11
413	Meso/micro-porosity and phase separation in TiO2/SiO2/C nanocomposites. Microporous and Mesoporous Materials, 2012, 150, 25-31.	4.4	11
414	Facile Deposition of Mesoporous PbI2 through DMF:DMSO Solvent Engineering for Sequentially Deposited Metal Halide Perovskites. ACS Applied Energy Materials, 2020, 3, 3358-3368.	5.1	11

#	Article	IF	CITATIONS
415	Origin of vertical slab orientation in blade-coated layered hybrid perovskite films revealed with in-situ synchrotron X-ray scattering. Nano Energy, 2021, 83, 105818.	16.0	11
416	Role of Nitrides in Oxynitride Glasses and Glassâ ́ Ceramics:  An NMR Investigation. Chemistry of Materials, 1996, 8, 2516-2522.	6.7	10
417	Infrared transmission of hot-pressed Y- and Dy-α-sialon ceramics. Materials Letters, 2004, 58, 1985-1988.	2.6	10
418	An alternative flexible electrode for dye-sensitized solar cells. Journal of Nanoparticle Research, 2012, 14, 1.	1.9	10
419	An over 10% enhancement of dye-sensitized solar cell efficiency by tuning nanoparticle packing. RSC Advances, 2013, 3, 17003.	3.6	10
420	Crystalline TiO ₂ Nanorod Aggregates: Templateâ€Free Fabrication and Efficient Light Harvesting in Dyeâ€6ensitized Solar Cell Applications. Particle and Particle Systems Characterization, 2013, 30, 754-758.	2.3	10
421	Controlled Growth of Monocrystalline Organoâ€Lead Halide Perovskite and Its Application in Photonic Devices. Angewandte Chemie, 2017, 129, 12660-12665.	2.0	10
422	Impact of Nickel Oxide/Perovskite Interfacial Contact on the Crystallization and Photovoltaic Performance of Perovskite Solar Cells. Solar Rrl, 2022, 6, .	5.8	10
423	Melt Intercalation of PMMA into Organically-Modified Layered Silicate. Materials Research Society Symposia Proceedings, 1999, 576, 137.	0.1	9
424	Phase assemblages of (Ca,Mg)-α-sialon ceramics derived from an α-sialon powder prepared by SHS. Journal of the European Ceramic Society, 2003, 23, 2343-2349.	5.7	9
425	Control of Microstructures in αâ€SiAlON Ceramics. Journal of the American Ceramic Society, 2002, 85, 276-278.	3.8	9
426	A novel in situ synthesis of SiBCN-Zr composites prepared by a sol–gel process and spark plasma sintering. Dalton Transactions, 2016, 45, 12739-12744.	3.3	9
427	Improving the intrinsic thermal stability of the MAPbI ₃ perovskite by incorporating cesium 5-aminovaleric acetate. RSC Advances, 2018, 8, 14991-14994.	3.6	9
428	Sub-sized monovalent alkaline cations enhanced electrical stability for over 17% hysteresis-free planar perovskite solar mini-module. Electrochimica Acta, 2019, 306, 635-642.	5.2	9
429	Low-Temperature Solution-Processed Amorphous Titania Nanowire Thin Films for 1 cm ² Perovskite Solar Cells. ACS Applied Materials & Interfaces, 2020, 12, 11450-11458.	8.0	9
430	Room-temperature Sputtered NiOx for hysteresis-free and stable inverted Cs-FA mixed-cation perovskite solar cells. Materials Science in Semiconductor Processing, 2020, 115, 105129.	4.0	9
431	3D nonlinear photolithography of Tin oxide ceramics via femtosecond laser. Science China Materials, 2021, 64, 1477-1484.	6.3	9
432	Ultrafast Growth of High-Quality Cs _{0.14} FA _{0.86} Pb(Br _{<i>x</i>} I _{1–<i>x</i>}) ₃ Thin Films Achieved Using Super-Close-Space Sublimation. ACS Applied Energy Materials, 2022, 5, 5797-5803.	5.1	9

#	Article	IF	CITATIONS
433	Preparation of dispersed zirconia barium aluminosilicate composites. Journal of the European Ceramic Society, 1995, 15, 787-794.	5.7	8
434	Chemical structure of composites derived from poly(silicic acid) and 2-hydroxyethylmethacrylate. Journal of Polymer Science Part A, 2001, 39, 1342-1352.	2.3	8
435	The Dependence of Benzo-15-Crown-5 Ether-Containing Oligo Paraphenylene Vinylene (CE-OPV) Emission Upon Complexation with Metal Ions in Solution. Journal of Fluorescence, 2003, 13, 427-436.	2.5	8
436	Slag Derived α-Sialon Ceramics and their Properties. Key Engineering Materials, 2004, 264-268, 781-786.	0.4	8
437	Charge Transport in Photoanodes Constructed with Mesoporous TiO ₂ Beads for Dye-Sensitized Solar Cells. Journal of Physical Chemistry C, 2014, 118, 16635-16642.	3.1	8
438	Ultra-fine zirconium diboride powders prepared by a combined sol–gel and spark plasma sintering technique. Journal of Sol-Gel Science and Technology, 2016, 77, 636-641.	2.4	8
439	Interfacial and Vacancies Engineering of Copper Nickel Sulfide for Enhanced Oxygen Reduction and Alcohols Oxidation Activity. Energy and Environmental Materials, 2023, 6, .	12.8	8
440	Regulating the Ni3+/Ni2+ ratio of NiOx by plasma treatment for fully vacuum-deposited perovskite solar cells. Materials Science in Semiconductor Processing, 2022, 148, 106839.	4.0	8
441	In-situ monitored chemical bath deposition of planar NiO layer for inverted perovskite solar cell with enhanced efficiency. Journal of Materials Science and Technology, 2023, 133, 145-153.	10.7	8
442	Anisotropic grain growth of R-α-sialon (R = Nd and Er). Journal of Materials Science, 2001, 36, 807-810.	3.7	7
443	Nano-Sized Bi ₄ Ti ₃ O ₁₂ Powder Prepared by the Hydrolysis Process. Key Engineering Materials, 2002, 224-226, 597-600.	0.4	7
444	Microwave calcination of thin TiO ₂ films on transparent conducting oxide glass substrates. Journal of Materials Science, 2004, 39, 6361-6363.	3.7	7
445	Study on the stability of Ce α-Sialon derived from SHS-ed powder. Journal of the European Ceramic Society, 2004, 24, 2853-2860.	5.7	7
446	Formation of AlNâ€Polytypoid Phases during α‣iAlON Decomposition. Journal of the American Ceramic Society, 1997, 80, 2459-2463.	3.8	7
447	Effects of starting composition and carbon content on the formation of CaALPHA. SiAlON powders by carbothermal reduction-nitridation. Journal of the Ceramic Society of Japan, 2010, 118, 827-829.	1.1	7
448	Charge Transport and Recombination in Dye-Sensitized Solar Cells on Plastic Substrates. Journal of Physical Chemistry C, 2014, 118, 15154-15161.	3.1	7
449	Bis(9,9-dihexyl-9H-fluorene-7-yl)amine (BDFA) as a new donor for porphyrin-sensitized solar cells. Organic Electronics, 2014, 15, 2448-2460.	2.6	7
450	Near-infrared absorbing porphyrin dyes with perpendicularly extended π-conjugation for dye-sensitized solar cells. RSC Advances, 2014, 4, 50897-50905.	3.6	7

#	Article	IF	CITATIONS
451	Surface plasma resonance enhanced photocurrent generation in NiO photoanode based solar cells. Materials Science and Engineering B: Solid-State Materials for Advanced Technology, 2015, 199, 1-8.	3.5	7
452	Efficient Gas Adsorption Using Superamphiphobic Porous Monoliths as the under-Liquid Gas-Conductive Circuits. ACS Applied Materials & Interfaces, 2019, 11, 24795-24801.	8.0	7
453	A novel dopant for spiro-OMeTAD towards efficient and stable perovskite solar cells. Science China Materials, 2021, 64, 2915-2925.	6.3	7
454	All-vacuum deposited perovskite solar cells with glycine modified NiO _{<i>x</i>} hole-transport layers. RSC Advances, 2022, 12, 10863-10869.	3.6	7
455	Mitigating the Internal Ion Migration of Organic–Inorganic Hybrid Perovskite by a Graphene Oxide Interlayer. ACS Applied Materials & Interfaces, 2022, 14, 22601-22606.	8.0	7
456	Microstructural Characterization of ZrO2/O'-SiAION Composites. Journal of the American Ceramic Society, 1996, 79, 1314-1318.	3.8	6
457	Thermal stability of mixed-cation α-sialon ceramics. Materials Science & Engineering A: Structural Materials: Properties, Microstructure and Processing, 2003, 339, 115-123.	5.6	6
458	Gelcasting of alumina ceramic in mixed PVP–HEMA systems. Advances in Applied Ceramics, 2004, 103, 257-260.	0.4	6
459	Control of fluorescence emission color of benzo 15-crown-5 ether substituted oligo phenylene vinylene–ceramic nanocomposites. Polymer, 2005, 46, 7176-7184.	3.8	6
460	Formation and Stability of βâ€Quartz Solidâ€Solution Phase in the Liâ€Siâ€Alâ€Oâ€N System. Journal of the American Ceramic Society, 1997, 80, 3045-3053.	3.8	6
461	Phase reactions in a hot pressed TiC/Si powder mixture. Ceramics International, 2012, 38, 1999-2003.	4.8	6
462	Musselâ€Directed Synthesis of Nitrogenâ€Doped Anatase TiO ₂ . Angewandte Chemie, 2016, 128, 3083-3087.	2.0	6
463	Microstructure and thermal shock behavior of sol–gel introduced ZrB2 reinforced SiBCN matrix. Journal of Sol-Gel Science and Technology, 2018, 86, 365-373.	2.4	6
464	Incorporation of Î ³ -butyrolactone (GBL) dramatically lowers the phase transition temperature of formamidinium-based metal halide perovskites. Chemical Communications, 2019, 55, 11743-11746.	4.1	6
465	Microstructure and mechanical properties of nanoscale SiC/Ca α-SiAlON composites. Journal of Materials Science, 1997, 32, 3263-3269.	3.7	5
466	Microstructure and property anisotropy of hot-pressed Ca α-sialon. Journal of Materials Science Letters, 2000, 19, 999-1002.	0.5	5
467	Effect of processing on toughness of Ca α-sialon ceramics. Journal of Materials Science, 2000, 35, 5817-5821.	3.7	5
468	The Effect of Processing Conditions on the Microstructures of α-SiAION Ceramics. Materials Science Forum, 2000, 325-326, 213-218.	0.3	5

#	Article	IF	CITATIONS
469	Rheological behavior of alumina aqueous suspension in acrylamide/polyacrylamide systems. Journal of Materials Science Letters, 2002, 21, 1163-1165.	0.5	5
470	Title is missing!. Journal of Materials Science, 2003, 38, 1359-1364.	3.7	5
471	Mechanical and erosion-resistance properties of slag $\hat{I}\pm$ -sialon ceramics. Journal of the European Ceramic Society, 2004, 24, 2847-2851.	5.7	5
472	A Power Management Architecture for Sensor Nodes. , 2007, , .		5
473	Influence of some selected organic molecules on intensity of luminescence of TiO2:Eu3+ electrodes. Journal of Luminescence, 2009, 129, 563-565.	3.1	5
474	Preparation of Ca-α SiAlON hollow spheres by carbothermal reduction–nitridation of CaO–Al2O3–SiO2 glass. Materials Letters, 2011, 65, 116-118.	2.6	5
475	Reversible α′↔β′ transformation in a textured Sm-sialon ceramic. Journal of the European Ceramic Society 2011, 31, 1165-1175.	, 5.7	5
476	Fabrication of high toughness alumina with elongated grains. Journal of Materials Science Letters, 2001, 20, 1425-1427.	0.5	4
477	Effect of processing on microstructure and optical properties of Dy-α-sialon. Materials Letters, 2004, 58, 3340-3344.	2.6	4
478	Preparation of ZrC Powder by Self-Propagating High-Temperature Synthesis. Advanced Materials Research, 2009, 66, 258-261.	0.3	4
479	Preparation of chemically sintered ZnO films and their application in dye sensitized solar cells formed on plastic substrates. Journal of Photochemistry and Photobiology A: Chemistry, 2012, 228, 15-21.	3.9	4
480	Morphology control of mesoporous silica-carbon nanocomposites via phase separation of poly(furfuryl alcohol) and silica in the sol–gel synthesis. Journal of Sol-Gel Science and Technology, 2017, 82, 664-674.	2.4	4
481	Visualisierung der Phasensegregation in Gemischthalogenid―Perowskiteinkristallen. Angewandte Chemie, 2019, 131, 2919-2924.	2.0	4
482	Bandgap adjustment assisted preparation of >18% Cs _y FA _{1â^'y} PbI _x Br _{3â^'x} -based perovskite solar cells using a hybrid spraying process. RSC Advances, 2021, 11, 17595-17602.	3.6	4
483	CsPb _{0.9} Sn _{0.1} IBr ₂ Based All-Inorganic Perovskite Solar Cells Exhibit Improved Efficiency and Stability. Wuli Huaxue Xuebao/ Acta Physico - Chimica Sinica, 2018, 34, 449-450.	4.9	4
484	Pressureless Sintering of Calcium Alpha Sialons. Materials Science Forum, 2000, 325-326, 199-206.	0.3	3
485	Preparation of High Concentrated Suspension and Gelcasting Process for Silicon Nitride Bonded Silicon Carbide Refractories. Key Engineering Materials, 2002, 224-226, 685-690.	0.4	3
486	Selective Laser Melting of Li ₂ 0.Al ₂ 0 ₃ .SiO ₂ (LAS) Glass Powders. Materials Science Forum, 2003, 437-438, 249-252.	0.3	3

#	Article	IF	CITATIONS
487	On the superstructure of KTiO2(OH). Zeitschrift Fur Kristallographie - Crystalline Materials, 2004, 219, 227-230.	0.8	3
488	Use of HEMA in Gelcasting of Ceramics: A Case Study on Fused Silica. Journal of the American Ceramic Society, 2006, 89, 060623005134011-???.	3.8	3
489	Enhanced charge collection in dye-sensitized solar cells utilizing collector–shell electrodes. Journal of Power Sources, 2015, 277, 343-349.	7.8	3
490	Post-Treatment of Photoanodes Including Mesoporous TiO2Beads in Dye-Sensitized Solar Cells Using Pulsed Deposition Technique. Journal of the Electrochemical Society, 2015, 162, H780-H784.	2.9	3
491	Perovskite Solar Cells: Effect of the Microstructure of the Functional Layers on the Efficiency of Perovskite Solar Cells (Adv. Mater. 20/2017). Advanced Materials, 2017, 29, .	21.0	3
492	Recovering Quadruple-cation Perovskite Films from Water Caused Permanent Degradations. Journal Wuhan University of Technology, Materials Science Edition, 2020, 35, 57-64.	1.0	3
493	Title is missing!. , 0, , .		3
494	Ionic liquid dopant for hole transporting layer towards efficient LiTFSI-free perovskite solar cells. Chemical Physics Letters, 2022, 801, 139713.	2.6	3
495	Densification of zirconia-containing sialon composites by Sm2O3. Journal of Materials Science, 1993, 28, 3097-3102.	3.7	2
496	Phase and microstructural evolution during the heat treatment of Sm–Ca–α-sialon ceramics. Journal of the European Ceramic Society, 2002, 22, 1609-1620.	5.7	2
497	Preparation of α-Sialon seed particles with different morphology. Journal of Materials Science Letters, 2002, 21, 589-591.	0.5	2
498	Microstructure control of α-Sialon ceramics by seeding with α-Sialon particles. Journal of Materials Science, 2002, 37, 3285-3290.	3.7	2
499	Formation behaviors of Sr0.4Ba0.6Nb2O6 powders synthesized from the molten salt of KCI. Journal of Materials Science Letters, 2003, 22, 949-951.	0.5	2
500	Properties of Aqueous Bismuth Titanate Suspensions Stabilized by Acrylic Acid/Acrylic Ester Copolymer. Journal of the American Ceramic Society, 2003, 86, 2203-2205.	3.8	2
501	Development of Textured Bismuth Titanate Piezoelectric Ceramics. Key Engineering Materials, 2003, 247, 371-376.	0.4	2
502	Preparation of Textured Bi ₄ Ti ₃ O ₁₂ Ceramics by Templated Grain Growth. Key Engineering Materials, 2004, 264-268, 1317-1320.	0.4	2
503	Effect of ratios of Y/Ce on phase assemblages of SHS-ed (Ce,Y) α-sialon powders and bulk materials. Materials Letters, 2004, 58, 3266-3270.	2.6	2
504	A New Route of Forming Silicon Carbide Nanostructures with Controlled Morphologies. Key Engineering Materials, 0, 403, 149-152.	0.4	2

#	Article	IF	CITATIONS
505	Creation of Titanium and Zirconium Carbide Fibers with the Forcespinning Technique. International Journal of Applied Ceramic Technology, 2016, 13, 619-628.	2.1	2
506	Solvent effects on adsorption kinetics, dye monolayer, and cell performance of porphyrin-sensitized solar cells. RSC Advances, 2016, 6, 114037-114045.	3.6	2
507	Recovering MAPbI ₃ -Based Perovskite Films From Water-Caused Permanent Degradations by Dipping in MAI Solution. IEEE Journal of Photovoltaics, 2018, 8, 1692-1700.	2.5	2
508	Printable materials for printed perovskite solar cells. Flexible and Printed Electronics, 2020, 5, 014002.	2.7	2
509	Scalable growth of stable wideâ€bandgap perovskite towards largeâ€scale tandem photovoltaics. Solar Rrl, 0, , .	5.8	2
510	Nonepitaxial heterogeneous nucleation of α-sialon in the Ca-doped system. Journal of Materials Research, 2001, 16, 578-582.	2.6	1
511	α′ phase stability in Nd–Li-sialon systems. Journal of the European Ceramic Society, 2003, 23, 1083-1092.	5.7	1
512	Synthesis of Ca- \hat{l} ± SiAlON Hollow Balls. Key Engineering Materials, 2003, 237, 87-94.	0.4	1
513	Microstructural Evidence for the Mechanism of the α↔β Phase Transformation in Ytterbium SiAlON Ceramics. Key Engineering Materials, 2003, 237, 157-162.	0.4	1
514	Novel Optical Ceramics: α-Sialons. Key Engineering Materials, 2004, 264-268, 905-908.	0.4	1
515	Phase Assemblages of Pr alpha-sialon Derived from SHS-ed Powders and TEM Study on the Nucleation of Pr alpha-sialon. Journal of the American Ceramic Society, 2005, 88, 950-953.	3.8	1
516	Eu stabilized α-sialon ceramics derived from SHS-synthesized powders. Materials Letters, 2005, 59, 205-209.	2.6	1
517	Effect of Microstructure on Sliding Wear of Ca α-SiAlON Ceramics. Key Engineering Materials, 2005, 280-283, 1253-1258.	0.4	1
518	An overview of the Australian Centre for Advanced Photovoltaics and the Australia-US Institute for Advanced Photovoltaics. Materials Research Society Symposia Proceedings, 2015, 1771, 33-44.	0.1	1
519	Aqueous Sn-S Complex Derived Electron Selective Layer for Perovskite Solar Cells. Journal Wuhan University of Technology, Materials Science Edition, 2020, 35, 272-279.	1.0	1
520	Hole-Conductor and Metal Electrode-Free Planar Perovskite Solar Cells. Current Nanoscience, 2015, 11, 494-498.	1.2	1
521	Fabrication and Performances of Flexible Monolithic Dye-sensitized Solar Cell Using Metal Reinforced Porous Counter Electrodes. Current Nanoscience, 2015, 11, 488-493.	1.2	1
522	Accelerated Crystal Growth in >16% Printed MA _{<i>x</i>} FA _{<i>y</i>} Cs _{<i>z</i>} Pbl ₃ Perovskite Solar Cells from Aqueous Inks. ACS Sustainable Chemistry and Engineering, 2022, 10, 5225-5232.	6.7	1

#	Article	IF	CITATIONS
523	Oxidation Behaviour of Zirconia-Sialon Composites. Materials Research Society Symposia Proceedings, 1992, 287, 527.	0.1	0
524	Zirconia Transformation in ZrO ₂ /O-Sialon Ceramic Composites. Materials Science Forum, 1995, 189-190, 393-398.	0.3	0
525	TEM observation on nucleation of Ca α-Sialon. Science Bulletin, 2001, 46, 216-219.	1.7	0
526	Effect of Dual Elements on Formation Behavior of Multi-Cation α-Sialons. Key Engineering Materials, 2002, 224-226, 257-262.	0.4	0
527	Microstructural Tailoring and Mechanical Properties of Ca α-Sialon Ceramics. Key Engineering Materials, 2002, 224-226, 251-256.	0.4	0
528	Suppression of Surface-Exfoliation by Gelcasting Ceramics with Mixed Polymer-Monomer Solutions. Key Engineering Materials, 2002, 224-226, 657-662.	0.4	0
529	Effect of .ALPHASi3N4 Addition on Sintering of MgALPHASiAlON Powders Journal of the Ceramic Society of Japan, 2002, 110, 1100-1102.	1.3	0
530	Densification of Ca-αSiAlON Nano Particles by Spark Plasma Sintering. Key Engineering Materials, 2003, 247, 71-74.	0.4	0
531	Application of Focused Ion Beam Miller in Fracture Characterization. Key Engineering Materials, 2003, 247, 297-300.	0.4	Ο
532	Synthesis of α-SiAlON from Slag by SHS and its Reaction Behavior. Key Engineering Materials, 2003, 247, 101-104.	0.4	0
533	The Role of Microstructure in the Erosion Behaviour of Engineering Ceramics. Key Engineering Materials, 2003, 237, 211-220.	0.4	0
534	Preferential Orientation of SiAlON Grains in Reversible α'↔β' Phase Transformations. Key Engineering Materials, 2003, 237, 163-168.	0.4	0
535	Comparison of the Luminescence Properties of Dy3+ in alpha-Sialon and Oxynitride Glass. Journal of the American Ceramic Society, 2005, 88, 2955-2956.	3.8	Ο
536	NANOSTRUCTURED TiO2 FILMS IN DYE-SENSITIZED SOLAR CELLS. International Journal of Nanoscience, 2005, 04, 785-793.	0.7	0
537	Sol-gel synthesis of TiO/sub 2/ nanocrystals for application in dye-sensitized solar cells. , 0, , .		Ο
538	A special issue on solar cells. Frontiers of Optoelectronics in China, 2011, 4, 1-1.	0.2	0
539	Prompting electron transport in mesoporous semiconductor electrode by simple film compression. International Journal of Nanotechnology, 2014, 11, 1006.	0.2	0
540	Perovskite Solar Cells: Solventâ€Mediated Dimension Tuning of Semiconducting Oxide Nanostructures as Efficient Charge Extraction Thin Films for Perovskite Solar Cells with Efficiency Exceeding 16% (Adv. Energy Mater. 7/2016). Advanced Energy Materials, 2016, 6, .	19.5	0

#	Article	IF	CITATIONS
541	Titelbild: Controlled Growth of Monocrystalline Organoâ€Lead Halide Perovskite and Its Application in Photonic Devices (Angew. Chem. 41/2017). Angewandte Chemie, 2017, 129, 12547-12547.	2.0	0
542	Molecular Engineering of Zinc-Porphyrin Sensitisers for p-Type Dye-Sensitised Solar Cells. ChemPlusChem, 2018, 83, 547-547.	2.8	0
543	Titelbild: Visualisierung der Phasensegregation in Gemischthalogenid―Perowskiteinkristallen (Angew.) Tj ETQq1	1 0,78431 2.0	4 rgBT /Ove
544	Chlorobenzenesulfonic Potassium Salts as the Efficient Multifunctional Passivator for the Buried Interface in Regular Perovskite Solar Cells (Adv. Energy Mater. 20/2022). Advanced Energy Materials, 2022, 12, .	19.5	0